Inorganic Chemistry
Article

Inorg. Chem. **2009**, *48*, 9325–9335 **9325**
DOI: 10.1021/ic901306k

Mn_4, Mn_6, and Mn_{11} Clusters from the Use of Bulky Diphenyl(pyridine-2-yl)methanol

Taketo Taguchi, Matthew R. Daniels, Khalil A. Abboud, and George Christou*

Department of Chemistry, University of Florida, Gainesville, Florida 32611-7200

Received July 6, 2009

The synthesis, crystal structure, and magnetochemical characterization are reported of three new Mn clusters $[Mn_4O_2(O_2CBu^t)_5(dphmp)_3]$ (**1**), $[Mn_6O_4(OMe)_2(O_2CPh)_4(dphmp)_4]$ (**2**), and $[Mn_{11}O_7(OMe)_7(O_2CPh)_7(dphmp)_4(MeOH)_2]$ (**3**). They were obtained from the use of diphenyl(pyridine-2-yl)methanol (dphmpH), a bulkier version of the 2-(hydroxymethyl)pyridine (hmpH) reagent commonly employed previously in Mn chemistry. The reaction of dphmpH with $MnCl_2 \cdot 4H_2O$ and NaO_2CBu^t in MeCN/MeOH (30 mL, 5:1 v/v) led to the isolation of tetranuclear complex **1**, whereas the analogous reaction with NaO_2CPh gave hexanuclear complex **2**. When the 5:1 solvent ratio in the latter reaction was changed to 1:29, the isolated product was now undecanuclear complex **3**. Complexes **1**−**3** all possess rare or unprecedented Mn_x topologies: Complex **1** possesses a $[Mn_4(\mu_3\text{-}O)_2]^{8+}$ ($4Mn^{III}$) butterfly core, one edge of which is additionally bridged by an alkoxide arm of a $dphmp^-$ chelate; complex **2** possesses a $[Mn_6(\mu_4\text{-}O)_2(\mu_3\text{-}O)_2(\mu_3\text{-}OMe)_2]^{8+}$ ($6Mn^{III}$) core with a face-sharing double cubane topology; and complex **3** (Mn^{II}, $10Mn^{III}$) possesses a $[Mn_4(\mu_4\text{-}O)_3(\mu_3\text{-}OMe)]^{5+}$ cubane unit, attached on one side to a Mn^{II} atom by a μ_4-O atom and alkoxide groups, and on the other side to a $[Mn_5(\mu_4\text{-}O)(\mu_3\text{-}O)_3(\mu_3\text{-}OMe)(\mu\text{-}OR)_3]^{3+}$ unit consisting of three face-sharing defective cubanes linked to an additional Mn^{III} atom by a μ_3-O atom. Solid-state dc and ac magnetic susceptibility measurements on **1**−**3** establish that they possess S = 0, 3, and 5/2 ground states, respectively. ac susceptibility studies on **2** and **3** reveal weak non-zero frequency-dependent out-of-phase (χ_M'') signals at temperatures below 3 K, possibly indicative of single-molecule magnets with very small barriers. The combined results demonstrate a ligating difference between bulky $dphmp^-$ and hmp^-, and the resulting usefulness of the former to provide access to a variety of Mn_x molecular species not known with the latter.

Introduction

There continues to be great interest in the synthesis and characterization of high-nuclearity 3d transition metal clusters. In some cases, this is because of their relevance to bioinorganic chemistry as models for the metallosites of various proteins and enzymes, whereas in other cases it is their importance to molecular magnetism that drives this interest. And in many instances, the intrinsic architectural beauty and the aesthetically pleasing structures of metal clusters are themselves the primary interest within the field of supramolecular chemistry.[1] In manganese chemistry, for example, Mn carboxylate clusters are of bioinorganic interest because of their relevance to elucidating the nature and mechanism of action of the water oxidizing complex (WOC) on the donor side of photosystem II in green plants and cyanobacteria.[2] The WOC comprises a pentanuclear Mn_4Ca cluster, whose exact structure is still unclear, and which is responsible for the light-driven, oxidative coupling of two molecules of water into dioxygen.[3] Second, some polynuclear Mn compounds have been found to be single-molecule magnets (SMMs), which are individual molecules capable of functioning as nanoscale magnetic particles and which thus represent a molecular approach to nanomagnetism.[4] Such molecules behave as magnets below their blocking temperature (T_B), exhibiting hysteresis in magnetization versus direct current (dc) field scans. This magnetic behavior of SMMs results from the combination of a large ground spin state (S) with a large and negative Ising (or easy-axis) type of magnetoanisotropy, as measured by the axial zero-field splitting parameter D. In addition, some of these molecules

*To whom correspondence should be addressed. E-mail: christou@chem.ufl.edu. Phone: +1-352-392-8314. Fax: +1-352-392-8757.

(1) Wang, X. J.; Langetepe, T.; Persau, C.; Kang, B.-S.; Sheldrick, G. M.; Fenske, D. *Angew. Chem., Int. Ed.* **2002**, *41*, 3818.

(2) (a) Ferreira, K. N.; Iverson, T. M.; Maghlaoui, K.; Barber, J.; Iwata, S. *Science* **2004**, *303*, 1831. (b) Carrell, T. G.; Tyryshkin, A. M.; Dismukes, G. C. *J. Biol. Inorg. Chem.* **2002**, *7*, 2. (c) Cinco, R. M.; Rompel, A.; Visser, H.; Aromi, G.; Christou, G.; Sauer, K.; Klein, M. P.; Yachandra, V. K. *Inorg. Chem.* **1999**, *38*, 5988. (d) Yachandra, V. K.; Sauer, K.; Klein, M. P. *Chem. Rev.* **1996**, *96*, 2927.

(3) (a) Law, N. A.; Caudle, M. T.; Pecoraro, V. L. In *Adv. Inorg. Chem.*; Sykes, A. G., Ed.; Academic Press: London, 1998; Vol. *46*, p 305. (b) Yocum, C. F.; Pecoraro, V. L. *Curr. Opin. Chem. Biol.* **1999**, *3*, 182.

(4) (a) Bagai, R.; Christou, G. *Chem. Soc. Rev.*, **2009**, *38*(4), 1011 and references cited therein. (b) Christou, G.; Gatteschi, D.; Hendrickson, D. N.; Sessoli, R. *MRS Bull.* **2000**, *25*, 66.

Published on Web 09/03/2009

have had remarkable structures, such as the giant Mn_{84} SMM with a torus structure.[5]

As a result of the above, we and others have explored and successfully developed many new routes for the synthesis of polynuclear Mn complexes, with nuclearities currently up to 84.[5] These procedures have included comproportionation reactions of simple starting materials,[6] reductive aggregation of permanganate ions,[7] aggregation of clusters of smaller nuclearity,[8] reductive aggregation or fragmentation of preformed clusters,[9] electrochemical oxidation,[10] and ligand substitution of preformed species,[11] among others. As part of this work, a wide variety of potentially chelating and/or bridging ligands have been explored to foster formation of high nuclearity products.[12−19] Among these are pyridyl alcohols, especially 2-(hydroxymethyl)pyridine (hmpH, Scheme 1),[19] which has proven to be an extremely versatile chelating and bridging group that has yielded a number of 3d metal clusters with various structural motifs, large *S* values, and SMM behavior. To explore new Mn cluster chemistry from such ligands, we have initiated a project in which the steric bulk of chelates such as hmpH has been increased by addition of bulky groups at positions that we expect to influence the identity of obtained cluster products. In the present work, we describe the use in Mn cluster chemistry of an hmpH derivative in which two bulky phenyl groups have been added onto the CH_2 unit. The resulting molecule, diphenyl-hmpH (dphmpH; IUPAC name is diphenyl (pyridine-2-yl)methanol) is shown in Scheme 1. We anticipated that the use of dphmpH in metal cluster chemistry would give products distinctly different from those with hmpH, and have therefore explored its use initially in Mn chemistry. Note that dphmpH has been previously employed only for the synthesis of mononuclear Zr, W, and Mo complexes.[20] In the present study, we have deliberately targeted higher nuclearity Mn products by exploring reactions between dphmpH and Mn^{II} salts under slightly basic conditions. This has successfully led to new Mn_4, Mn_6, and Mn_{11} clusters, and their syntheses, structures, and magnetochemical characterization are described in this paper.

Scheme 1

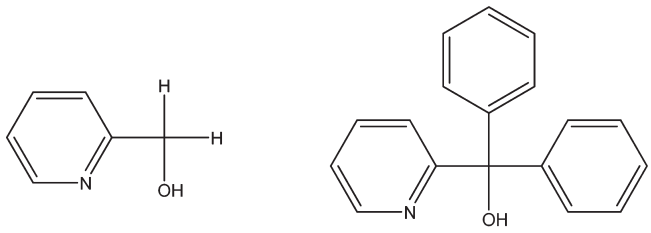

hmpH **dphmpH**

Experimental Section

Syntheses. All preparations were performed under aerobic conditions except for the synthesis of dmhmpH, which was

(5) Tasiopoulos, A. J.; Vinslava, A.; Wernsdorfer, W.; Abboud, K. A.; Christou, G. *Angew. Chem., Int. Ed.* **2004**, *43*, 2117.

(6) For example, see: (a) Price, D. J.; Batten, S. R.; Moubaraki, B.; Murray, K. S. *Chem. Commun.* **2002**, 762. (b) Milios, C. J.; Raptopoulou, C. P.; Terzis, A.; Lloret, F.; Vicente, R.; Perlepes, S. P.; Escuer, A. *Angew. Chem., Int. Ed.* **2003**, *43*, 210. (c) Murugesu, M.; Habrych, M.; Wernsdorfer, W.; Abboud, K. A.; Christou, G. *J. Am. Chem. Soc.* **2004**, *126*, 4766.

(7) (a) Tasiopoulos, A. J.; Wernsdorfer, W.; Abboud, K. A.; Christou, G. *Angew. Chem., Int. Ed.* **2004**, *43*, 6338. (b) King, P.; Wernsdorfer, W.; Abboud, K. A.; Christou, G. *Inorg. Chem.* **2004**, *43*, 7315. (c) Tasiopoulos, A. J.; Wernsdorfer, W.; Abboud, K. A.; Christou, G. *Inorg. Chem.* **2005**, *44*, 6324.

(8) For example, see: (a) Maheswaran, S.; Chastanet, G.; Teat, S. J.; Mallah, T.; Sessoli, R.; Wernsdorfer, W.; Winpenny, R. E. P. *Angew. Chem., Int. Ed.* **2005**, *44*, 5044. (b) Wu, Q.; Li, Y.-G.; Wang, Y.-H.; Wang, E.-B.; Zhang, Z.-M.; Clerac, R. *Inorg. Chem.* **2009**, *48*, 1606. (c) Scott, R. T. W.; Parsons, S.; Murugesu, M.; Wernsdorfer, W.; Christou, G.; Brechin, E. K. *Angew. Chem., Int. Ed.* **2005**, *44*, 6540.

(9) (a) Manoli, M.; Prescimone, A.; Mishra, A.; Parsons, S.; Christou, G.; Brechin, E. K. *Dalton Trans.* **2007**, 532. (b) Bhaduri, S.; Tasiopoulos, A.; Pink, M.; Abboud, K. A.; Christou, G. *Chem. Commun.* **2002**, 2352.

(10) (a) Aliaga-Alcalde, N.; Edwards, R. S.; Hill, S. O.; Wernsdorfer, W.; Folting, K.; Christou, G. *J. Am. Chem. Soc.* **2004**, *126*, 12503. (b) Wang, S.; Wemple, M. S.; Tsai, H.-L.; Folting, K.; Huffman, J. C.; Hagen, K. S.; Hendrickson, D. N.; Christou, G. *Inorg. Chem.* **2000**, *39*, 1501. (c) Wang, S.; Tsai, H.-L.; Hagen, K. S.; Hendrickson, D. N.; Christou, G. *J. Am. Chem. Soc.* **1994**, *116*, 8376.

(11) (a) Eppley, H. J.; Tsai, H.-L.; de Vries, N.; Folting, K.; Christou, G.; Hendrickson, D. N. *J. Am. Chem. Soc.* **1995**, *117*, 301. (b) Eppley, H. J.; Christou, G.; Law, N. A.; Pecoraro, V. L. *Inorg. Synth.* **2002**, *33*, 61. (c) Chakov, N. E.; Zakharov, L. N.; Rheingold, A. L.; Abboud, K. A.; Christou, G. *Inorg. Chem.* **2005**, *44*, 4555.

(12) (a) Brechin, E. K.; Soler, M.; Christou, G.; Helliwell, M.; Teat, S. J.; Wernsdorfer, W. *Chem. Commun.* **2003**, 1276. (b) Rajaraman, G.; Murugesu, M.; Soler, M.; Wernsdorfer, W.; Helliwell, M.; Teat, S. J.; Christou, G.; Brechin, E. K. *J. Am. Chem. Soc.* **2004**, *126*, 15445. (c) Piligkos, S.; Rajaraman, G.; Soler, M.; Kirchner, N.; van Slageren, J.; Bircher, R.; Parsons, S.; Güdel, H.-U.; Kortus, J.; Wernsdorfer, W.; Christou, G.; Brechin, E. K. *J. Am. Chem. Soc.* **2005**, *127*, 5572.

(13) (a) Milios, C. J.; Vinslava, A.; Wernsdorfer, W.; Moggach, S.; Parsons, S.; Perlepes, S. P.; Christou, G.; Brechin, E. K. *J. Am. Chem. Soc.* **2007**, *129*, 2754. (b) Milios, C. J.; Vinslava, A.; Wernsdorfer, W.; Prescimone, A.; Wood, P. A.; Parsons, S.; Perlepes, S. P.; Christou, G.; Brechin, E. K. *J. Am. Chem. Soc.* **2007**, *129*, 6547. (c) Milios, C. J.; Inglis, R.; Vinslava, A.; Bagai, R.; Wernsdorfer, W.; Parsons, S.; Perlepes, S. P.; Christou, G.; Brechin, E. K. *J. Am. Chem. Soc.* **2007**, *129*, 12505.

(14) (a) Foguet-Albiol, D.; O'Brien, T. A.; Wernsdorfer, W.; Moulton, B.; Zaworotko, M. J.; Abboud, K. A.; Christou, G. *Angew. Chem., Int. Ed.* **2005**, *44*, 897. (b) Saalfrank, R. W.; Nakajima, T.; Mooren, N.; Scheurer, A.; Maid, H.; Hampel, F.; Trieflinger, C.; Daub, J. *Eur. J. Inorg. Chem.* **2005**, 1149. (c) Rumberger, E. M.; Shah, S. J.; Beedle, C. C.; Zakharov, L. N.; Rheingold, A. L.; Hendrickson, D. N. *Inorg. Chem.* **2005**, *44*, 2742.

(15) (a) Murugesu, M.; Wernsdorfer, W.; Abboud, K. A.; Christou, G. *Angew. Chem., Int. Ed.* **2005**, *44*, 892. (b) Wittick, L. M.; Jones, L. F.; Jensen, P.; Moubaraki, B.; Spiccia, L.; Berry, K. J.; Murray, K. S. *Dalton Trans.* **2006**, 1534. (c) Wittick, L. M.; Murray, K. S.; Moubaraki, B.; Batten, S. R.; Spiccia, L.; Berry, K. J. *Dalton Trans.* **2004**, 1003.

(16) (a) Ako, A. M.; Hewitt, I. J; Mereacre, V.; Clérac, R.; Wernsdorfer, W.; Anson, C. E.; Powell, A. K. *Angew. Chem., Int. Ed.* **2006**, *45*, 4926. (b) Moushi, E. E.; Stamatatos, Th. C.; Wernsdorfer, W.; Nastopoulos, V.; Christou, G.; Tasiopoulos, A. J. *Inorg. Chem.* **2009**, *48*, 5049. (c) Nayak, S.; Lan, Y.; Clérac, R.; Ansona, C. E.; Powell, A. K. *Chem. Commun.* **2008**, 5698.

(17) (a) Stamatatos, Th. C.; Foguet-Albiol, D.; Stoumpos, C. C.; Raptopoulou, C. P.; Terzis, A.; Wernsdorfer, W.; Perlepes, S. P.; Christou, G. *J. Am. Chem. Soc.* **2005**, *127*, 15380. (b) Stamatatos, Th. C.; Foguet-Albiol, D.; Lee, S. C.; Stoumpos, C. C.; Raptopoulou, C. P.; Terzis, A.; Wernsdorfer, W.; Hill, S.; Perlepes, S. P.; Christou, G. *J. Am. Chem. Soc.* **2007**, *129*, 9484. (c) Goldberg, D. P.; Caneschi, A.; Lippard, S. J. *J. Am. Chem. Soc.* **1993**, *115*, 9299. (d) Goldberg, D. P.; Caneschi, A.; Delfs, C. D.; Sessoli, R.; Lippard, S. J. *J. Am. Chem. Soc.* **1995**, *117*, 5789.

(18) (a) Milios, C. J.; Kefalloniti, E.; Raptopoulou, C. P.; Terzis, A.; Vicente, R.; Lalioti, N.; Escuer, A.; Perlepes, S. P. *Chem. Commun.* **2003**, 819. (b) Zaleski, C. M.; Depperman, E. C.; Dendrinou-Samara, C.; Alexiou, M.; Kampf, J. W.; Kessissoglou, D. P.; Kirk, M. L.; Pecoraro, V. L. *J. Am. Chem. Soc.* **2005**, *127*, 12862. (c) Stamatatos, Th. C.; Abboud, K. A.; Wernsdorfer, W.; Christou, G. *Angew. Chem., Int. Ed.* **2008**, *47*, 6694.

(19) (a) Harden, N. C.; Bolcar, M. A.; Wernsdorfer, W.; A. Abboud, K.; Streib, W. E.; Christou, G. *Inorg. Chem.* **2003**, *42*, 7067. (b) Bolcar, M. A.; Aubin, S. M. J.; Folting, K.; Hendrickson, D. N. *Chem. Commun.* **1997**, 1485.

(20) (a) Doherty, S.; Errington, R. J.; Jarvis, A. P.; Collins, S.; Clegg, W.; Elsegood, M. R. J. *Organometallics* **1998**, *17*, 3408. (b) Schltz, B. E.; Gheller, S. F.; Muetterties, M. C.; Scott, M. J.; Holm, R. H. *J. Am. Chem. Soc.* **1993**, *115*, 2714. (c) Wong, Y.-L.; Yang, Q.; Zhou, Z.-Y.; Lee, H. K.; Mak, T. C. W.; Ng, D. K. P. *New J. Chem.* **2001**, *25*, 353.

carried out as previously reported.[21] All chemicals were used as received.

[$Mn_4O_2(O_2CBu^t)_5(dphmp)_3$] (1). To a stirred solution of dphmpH (0.26 g, 1.0 mmol) and NEt_3 (0.42 mL, 3.0 mmol) in MeCN/MeOH (30 mL, 5:1 v/v) was added solid $MnCl_2 \cdot 4H_2O$ (0.20 g, 1.0 mmol) and $NaO_2CBu^t \cdot H_2O$ (0.25 g, 2.0 mmol). The mixture was stirred overnight, filtered to remove NaCl, and the filtrate layered with Et_2O (60 mL). X-ray quality crystals of **1**·2MeCN slowly grew over 5 days in 55% yield. These were collected by filtration, washed with cold MeCN (2 × 3 mL) and Et_2O (2 × 5 mL), and dried under vacuum. Anal. Calcd (Found) for **1**·2MeCN·H_2O ($C_{83}H_{93}N_5Mn_4O_{15}$): C, 61.52 (61.10); H, 5.78 (5.99); N, 4.32 (3.93). Selected IR data (cm^{-1}): 3446(mb), 3059(w), 3020(w), 2956(m), 2926(m), 2896(w), 2867(w), 2361(m), 2337(m), 1603(s), 1578(m), 1564(s), 1481(s), 1445(w), 1406(s), 1369(m), 1356(m), 1224(m), 1168(w), 1111(w), 1082(w), 1402(m), 1024(m), 953(w), 930(w), 907(w), 891(w), 778(m), 750(w), 703(m), 683(m), 659(m), 648(m), 635(m), 607(m), 597(m), 541(w), 525(w), 492(w), 463(w), 434(m).

[$Mn_6O_4(OMe)_2(O_2CPh)_4(dphmp)_4$] (2). Method A. To a stirred solution of dphmpH (0.26 g, 1.0 mmol) and NEt_3 (0.42 mL, 3.0 mmol) in MeCN/MeOH (30 mL, 5:1 v/v) was added solid $Mn(O_2CPh)_2$ (0.33 g, 1.0 mmol). The resulting dark brown solution was stirred overnight, filtered, and the filtrate left undisturbed to concentrate slowly by evaporation. X-ray quality crystals of **2**·3MeCN slowly grew over 2 weeks in 20% yield. These were collected by filtration, washed with cold MeCN (2 × 3 mL) and Et_2O (2 × 5 mL), and dried under vacuum. Anal. Calcd (Found) for **2**·2H_2O ($C_{120}H_{86}N_4Mn_6O_{20}$): C, 60.73 (60.51); H, 4.30 (3.96); N, 2.78 (3.09). Selected IR data (cm^{-1}): 3415(mb), 3057(w), 2935(w), 2739(w), 2677(w), 2491(w), 1598(s), 1561(s), 1489(w), 1475(w), 1445(w), 1389(s), 1251(w), 1170(m), 1044(m), 1024(m), 951(w), 928(w), 910(w), 841(w), 774(m), 707(m), 681(m), 661(m), 633(m), 607(m), 582(m), 529(m), 461(w), 433(w).

Method B. To a stirred solution of dphmpH (0.26 g, 1.0 mmol) and NEt_3 (0.42 mL, 3.0 mmol) in MeCN/MeOH (30 mL, 5:1 v/v) was added solid $MnCl_2 \cdot 4H_2O$ (0.20 g, 1.00 mmol) and NaO_2CPh (0.29 g, 2.00 mmol). The mixture was stirred overnight, filtered to remove NaCl, and the filtrate left undisturbed to concentrate slowly by evaporation. X-ray quality crystals of **2**·3MeCN slowly grew over 2 weeks in 15% yield. These were collected by filtration, washed with cold MeCN (2 × 3 mL) and Et_2O (2 × 5 mL), and dried under vacuum; the product was identified by IR spectral comparison as identical with material from Method A.

[$Mn_{11}O_7(OMe)_7(O_2CPh)_7(dphmp)_4(MeOH)_2$] (3). Method A. To a stirred solution of dphmpH (0.26 g, 1.0 mmol) and NEt_3 (0.42 mL, 3.0 mmol) in MeCN/MeOH (30 mL, 1:29 v/v) was added solid $Mn(O_2CPh)_2$ (0.33 g, 1.0 mmol). The resulting dark brown solution was stirred overnight, filtered, and the filtrate left undisturbed to concentrate slowly by evaporation. X-ray quality crystals of **3**·4MeCN slowly grew over 2 weeks in 25% yield. These were collected by filtration, washed with cold MeCN (2 × 3 mL) and Et_2O (2 × 5 mL), and dried under vacuum. Dried solid analyzed as solvent-free. Anal. Calcd (Found) for **3** ($C_{130}H_{120}N_4Mn_{11}O_{34}$): C, 54.09 (53.89); H, 4.19 (3.98); N, 1.94 (1.91). Selected IR data (cm^{-1}): 3417(mb), 3059(w), 2919(w), 2809(w), 1598(s), 1557(s), 1490(w), 1474(w), 1445(w), 1390(s), 1252(w), 1171(w), 1048(m), 953(w), 930(w), 910(w), 836(w), 773(w), 706(m), 680(m), 680(m), 657(w), 634(m), 592(m), 565(m), 468(w), 425(w).

Method B. To a stirred solution of dphmpH (0.26 g, 1.0 mmol) and NEt_3 (0.42 mL, 3.0 mmol) in MeCN/MeOH (30 mL, 1:29 v/v) was added solid $MnCl_2 \cdot 4H_2O$ (0.20 g, 1.0 mmol) and NaO_2CPh (0.29 g, 2.0 mmol). The mixture was stirred overnight, filtered to remove NaCl, and the filtrate left undisturbed to concentrate slowly by evaporation. X-ray quality crystals of **2**·3MeCN slowly grew over 2 weeks in 20% yield. These were collected by filtration, washed with cold MeCN (2 × 3 mL) and Et_2O (2 × 5 mL), and dried under vacuum; the product was identified by IR spectral comparison as identical with material from Method A.

X-ray Crystallography. Data were collected on a Siemens SMART PLATFORM equipped with a CCD area detector and a graphite monochromator utilizing Mo Kα radiation (λ = 0.71073 Å). Suitable crystals of **1**·2MeCN, **2**·3MeCN, and **3**·4MeCN were attached to glass fibers using silicone grease and transferred to a goniostat where they were cooled to 173 K for data collection. Cell parameters were refined using up to 8192 reflections. A full sphere of data (1850 frames) was collected using the ω-scan method (0.3° frame width). The first 50 frames were remeasured at the end of data collection to monitor instrument and crystal stability (maximum correction on I was <1%). Absorption corrections by integration were applied based on measured indexed crystal faces. The structure was solved by Direct Methods in SHELXTL6,[22] and refined on F^2 using full-matrix least-squares. The non-H atoms were treated anisotropically, whereas the H atoms were calculated in ideal positions and refined as riding on their respective C atoms.

For **1**·2MeCN, the asymmetric unit contains the Mn_4 cluster and two MeCN molecules. A total of 979 parameters were refined in the final least-squares cycle using 14826 reflections with $I > 2\sigma(I)$ to yield R_1 and wR_2 of 6.28 and 15.09%, respectively. In **2**·3MeCN, the asymmetric unit contains two half Mn_6 clusters, and three MeCN molecules. The latter were disordered and could not be modeled properly; thus, program SQUEEZE,[23] a part of the PLATON package of crystallographic software, was used to calculate the solvent disorder area and remove its contribution to the overall intensity data. A total of 1171 parameters were refined in the final least-squares cycle using 6680 reflections with $I > 2\sigma(I)$ to yield R_1 and wR_2 of 8.07 and 18.53%, respectively. For **3**·4MeCN, the asymmetric unit contains the Mn_{11} cluster and four MeCN molecules. The latter were disordered and could not be modeled properly; thus, program SQUEEZE was again used to calculate the solvent disorder area and remove its contribution to the overall intensity data. The O22 position of the Mn_{11} cluster is disordered between an OH and a methoxy group. The protons of the two coordinated MeOH groups were obtained from a difference Fourier map and refined freely. A total of 1637 parameters were refined in the final least-squares cycle using 12365 reflections with $I > 2\sigma(I)$ to yield R_1 and wR_2 of 5.66 and 10.18%, respectively.

Unit cell data and details of the structure refinements for the three complexes are collected in Table 1.

Other Studies. Infrared spectra were recorded in the solid state (KBr pellets) on a Nicolet Nexus 670 FTIR spectrometer in the 400−4000 cm^{-1} range. Elemental analyses (C, H, and N) were performed by the in-house facilities of the University of Florida, Chemistry Department. Variable-temperature dc and alternating current (ac) magnetic susceptibility data were collected on a Quantum Design MPMS-XL SQUID susceptometer equipped with a 7 T magnet and operating in the 1.8−300 K range. Samples were embedded in solid eicosane to prevent torquing. Magnetization versus field and temperature data was fit using the program MAGNET. Pascal's constants[24] were used to estimate the diamagnetic corrections, which were subtracted

(21) Tzerpos, N. I.; Zarkadis, A. K.; Kreher, R. P.; Repas, L.; Lehnig, M. *J. Chem. Soc., Perkin Trans. 2* **1995**, *4*, 755.

(22) *SHELXTL6*; Bruker-AXS: Madison, WI, 2000.

(23) Van der Sluis, P.; Spek, A. L. *Acta Crystallogr., Sect. A: Found. Crystallogr.* **1990**, *A46*, 194.

(24) *CRC handbook of Chemistry and Physics*; Weast, R. C., Ed.; CRC Press, Inc.: Boca Raton, FL1984.

Table 1. Crystallographic Data for **1**·2MeCN, **2**·3MeCN, and **3**·4MeCN

	1	2	3
formula[a]	$C_{83}H_{93}Mn_4N_5O_{15}$	$C_{108}H_{96}Mn_6N_7O_{18}$	$C_{138}H_{133}Mn_{11}N_8O_{34}$
fw, g mol^{-1}[a]	1620.38	2019.56	3051.86
crystal system	triclinic	triclinic	triclinic
space group	$P\bar{1}$	$P\bar{1}$	$P\bar{1}$
a, Å	13.1020(16)	13.5311(19)	17.0807(15)
b, Å	13.6590(17)	13.6589(18)	18.5090(16)
c, Å	14.6292(18)	27.034(4)	21.0431(18)
α, deg	63.067(2)	98.178(3)	94.9260(10)
β, deg	63.803(2)	90.914(3)	93.104(2)
γ, deg	65.072(2)	105.032(3)	96.2410(10)
V, Å^3	2012.4(4)	4769.1(11)	6575.3(10)
Z	1	2	2
T, K	173(2)	173(2)	173(2)
radiation, Å[b]	0.71073	0.71073	0.71073
ρ_{calc}, g cm^{-3}	1.337	1.469	1.541
μ, mm^{-1}	0.680	0.845	1.100
$R1$[c,d]	0.0628	0.0807	0.0566
$wR2$[e]	0.1509	0.1853	0.1018

[a] Including solvate molecules. [b] Graphite monochromator. [c] $I > 2\sigma(I)$. [d] $R1 = \sum||F_o| - |F_c||/\sum|F_o|$. [e] $wR2 = [\sum w(F_o^2 - F_c^2)^2/\sum w(F_o^2)^2]^{1/2}$, $w = 1/[\sigma^2(F_o^2) + [(ap)^2 + bp]$, where $p = [\max(F_o^2, 0) + 2F_c^2]/3$.

from the experimental susceptibilities to give the molar paramagnetic susceptibility (χ_M).

Results and Discussion

Syntheses. To make clusters containing Mn^{III} ions, one strategy is to oxidize simple Mn^{II} salts by atmospheric O_2 under prevailing basic conditions in the presence of potentially chelating ligands. In hmpH chemistry, this strategy has led to the isolation of a series of clusters possessing an $[Mn_4(hmp)_6]^{4+}$ core.[25,26] Therefore, we decided to also employ this strategy with the bulkier derivative dphmpH, and a variety of reaction ratios, reagents, and other conditions were investigated before the following procedures were developed. The reaction of dphmpH with $MnCl_2\cdot 4H_2O$, $NaO_2CBu^t\cdot H_2O$, and NEt_3 in 1:1:2:3 ratio in MeCN/MeOH (5:1) afforded a brown solution from which was subsequently obtained the tetranuclear complex $[Mn_4O_2(O_2CBu^t)_5(dphmp)_3]$ in 55% yield; the mixed solvent system was used to ensure adequate solubility of all reagents. The formation of **1** is summarized in eq 1, assuming atmospheric O_2 is

$$4Mn^{2+} + 5Bu^tCO_2^- + 3dphmpH + 3NEt_3 + O_2 \rightarrow [Mn_4O_2(O_2CBu^t)_5(dphmp)_3] + 3NHEt_3^+ \quad (1)$$

the oxidizing agent. Small variations in the Mn/dphmpH/$Bu^tCO_2^-$ ratio still gave complex **1**, which clearly is a preferred product of these components and with pivalate. We also employed other Mn salts, for example, NO_3^- or ClO_4^-, but again obtained complex **1** in every case. We then investigated the identity of product as a function of carboxylate groups.

The reaction of dphmpH with $Mn(O_2CPh)_2$ and NEt_3 in a 1:1:3 ratio in MeCN/MeOH (5:1) gave a brown solution from which was subsequently isolated $[Mn_6O_4(OMe)_2(O_2CPh)_4(dphmp)_4]$ (**2**) in 20% yield (Method A). The similar reaction of dphmpH with $MnCl_2\cdot 4H_2O$, NaO_2CPh, and NEt_3 in 1:1:2:3 ratio in MeCN/MeOH (5:1) also gave **2** in a slightly lower yield of 15% (Method B). Its formation via Method A is summarized in eq 2. Increasing or decreasing the amount of dphmpH also gave complex **2**, but the product

$$6Mn(O_2CPh)_2 + 4dphmpH + H_2O + 2MeOH + 3/2O_2 \rightarrow [Mn_6O_4(OMe)_2(O_2CPh)_4(dphmp)_4] + 8PhCO_2H \quad (2)$$

was not as pure. The low yield of the reaction clearly indicates, as with many other reactions in Mn^{III} chemistry, that the reaction solution probably contains a complicated mixture of several species in equilibrium, with factors such as relative solubility, lattice energies, crystallization kinetics, and others determining the identity of the product that crystallizes. One (or more) of these factors is undoubtedly the reason that changing the carboxylate used from pivalate to benzoate causes a major change in the identity of the product from **1** to **2**. Along these lines, it is worth noting that we were unable to isolate any pure product from the use of $Mn(O_2CMe)_2\cdot 4H_2O$ in an otherwise identical reaction system.

We also investigated the identity of the product as a function of the solvent composition. When the reaction that gives **2** was carried out with less MeOH, the product was still **2** but in an appreciably lower yield. However, at the other extreme, when the reaction was performed in predominantly MeOH, namely, MeCN/MeOH (1:29), the undecanuclear complex $[Mn_{11}O_7(OMe)_7(O_2CPh)_7(dphmp)_4(MeOH)_2]$ (**3**) was obtained in 25% yield. The small amount of MeCN was found beneficial in obtaining well-formed, X-ray quality crystals. Unlike **1** and **2**,

(25) (a) Yoo, J.; Yamaguchi, A.; Nakano, M.; Krzystek, J.; Streib, W. E.; Brunel, L.-C.; Ishimoto, H.; Christou, G.; Hendrickson, D. N. *Inorg. Chem.* **2001**, *40*, 4604. (b) Lecren, L.; Roubeau, O.; Li, Y.-G.; Le Goff, X. F.; Miyasaka, H.; Richard, F.; Wernsdorfer, W.; Coulon, C.; Clérac, R. *Dalton Trans.* **2008**, 755. (c) Miyasaka, H.; Nakata, K.; Lecren, L.; Coulon, C.; Nakazawa, Y.; Fujisaki, T.; Sugiura, K.; Yamashita, M.; Clérac, R. *J. Am. Chem. Soc.* **2006**, *128*, 3770.

(26) (a) Lecren, L.; Wernsdorfer, W.; Li, Y.-G.; Roubeau, O.; Miyasaka, H.; Clerac, R. *J. Am. Chem. Soc.* **2005**, *127*, 11311. (b) Lecren, L.; Li, Y.-G.; Wernsdorfer, W.; Roubeau, O.; Miyasaka, H.; Clerac, R. *Inorg. Chem. Commun.* **2005**, *8*, 626. (c) Lecren, L.; Roubeau, O.; Coulon, C.; Li, Y.-G.; Le Goff, X. F.; Wernsdorfer, W.; Miyasaka, H.; Clerac, R. *J. Am. Chem. Soc.* **2005**, *127*, 17353.

complex **3** is mixed-valent (Mn^{II}, 10 Mn^{III}), and its formation is summarized in eq 3.

$$11Mn(O_2CPh)_2 + 4dphmpH + 15NEt_3 + 9MeOH + 2H_2O + 5/2O_2 \rightarrow [Mn_{11}O_7(OMe)_7(O_2CPh)_7(dphmp)_4(MeOH)_2] + 15PhCO_2^- + 15NHEt_3^+ \quad (3)$$

The use of a mixed MeCN/EtOH solvent system instead of MeCN/MeOH led to the known, dphmpH-free clusters $[Mn_6(O_2CPh)_{10}(EtOH)_4(H_2O)]$ or $[Mn_{13}O_8(OEt)_6(O_2CPh)_{12}]$, depending on the exact solvent ratios.[27]

Description of Structures. The partially labeled structure of $[Mn_4O_2(O_2CBu^t)_5(dphmp)_3]$ (**1**) is shown in Figure 1; selected interatomic distances and angles are listed in Table 2. Complex **1** crystallizes in the rare triclinic space group $P\bar{1}$ and possesses a near-planar Mn_4 unit bridged by μ_3-O^{2-} ions O1 and O2 above and below the Mn_4 plane. A $[Mn_4(\mu_3\text{-}O)_2]^{8+}$ core containing an exactly planar Mn_4 rhombus is what we have described as a "planar butterfly" unit in the past,[28] to emphasize its relationship to the related $[Mn_4O_2]^{8+}$ complexes with a true butterfly (i.e., V-shaped) Mn_4 topology, such as that in the hmp^- cluster anion $[Mn_4O_2(O_2CPh)_7(hmp)_2]^-$ (**4**) with virtual C_2 symmetry.[29] In both the butterfly and planar-butterfly complexes obtained previously, including **4**, each Mn_2 edge of the $[Mn_4(\mu_3\text{-}O)_2]$ core is bridged by one or two carboxylate groups and each "wingtip" Mn atom is chelated by a bidentate ligand. The butterfly versus planar-butterfly difference is caused by the presence or absence, respectively, of a $\eta^1{:}\eta^1{:}\mu$−carboxylate group bridging the two central ("body") Mn atoms. Complex **1** is overall similar to these previous complexes in possessing a $dphmp^-$ chelate on wingtip atoms Mn1 and Mn2, and bridging $Bu^tCO_2^-$ groups, but differs in having an unusually low symmetry as a result of (i) possessing a third $dphmp^-$ group in a $\eta^1{:}\eta^2{:}\mu$ bridging mode, chelating "body" atom Mn3 and bridging to Mn2 with its deprotonated alkoxide arm in a very asymmetric manner (Mn3−O5 = 1.887(3) Å vs Mn2−O5 = 2.505(3) Å); and (ii) the carboxylate group bridging Mn2 and Mn4 also bonds weakly to Mn3 (Mn3−O12 = 2.784(3) Å vs Mn4−O12 = 2.282(3) Å) and is thus in an approximately $\eta^2{:}\eta^1{:}\mu_3$ binding mode. As a result, the Mn_4 topology of **1** is intermediate between the true planar-butterfly and V-shaped butterfly topologies observed previously. Charge considerations and the metric parameters indicate all Mn atoms to be Mn^{III}, as confirmed by BVS calculations[30] (Table 3). All Mn atoms are six-coordinate with near-octahedral geometries, and undergo the expected Jahn−Teller (JT) axial elongation; the elongation axes at Mn2 and Mn3 contain the long bonds mentioned above, with O12 also lying on the JT elongation axis of Mn4. For Mn1, the JT axis is O6−Mn1−O8.

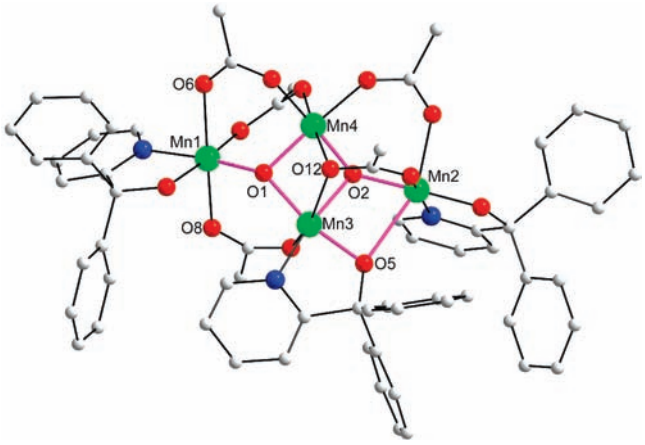

Figure 1. Structure of complex **1**, with core Mn−O bonds shown in purple. Hydrogen atoms and methyl groups on pivalates have been omitted for clarity. Color code: Mn^{III} green; O red; N blue; C gray.

Table 2. Selected Interatomic Distances (Å) and Angles (deg) for **1**·2MeCN

Mn1−O3	1.867(3)	Mn3−N3	2.021(4)
Mn1−O1	1.899(3)	Mn3−O9	2.101(3)
Mn1−O14	1.965(3)	Mn3···Mn4	2.7412(9)
Mn1−N1	2.053(4)	Mn4−O1	1.898(3)
Mn1−O8	2.193(3)	Mn4−O2	1.903(3)
Mn1−O6	2.219(3)	Mn4−O7	1.931(3)
Mn2−O4	1.861(3)	Mn4−O10	1.970(3)
Mn2−O2	1.887(3)	Mn4−O15	2.153(3)
Mn2−O13	1.974(3)	Mn4−O12	2.282(3)
Mn2−N2	2.049(4)	Mn4−O1−Mn1	120.15(16)
Mn2−O11	2.151(3)	Mn4−O1−Mn3	92.25(13)
Mn2−O5	2.505(3)	Mn1−O1−Mn3	130.31(17)
Mn2···Mn3	3.1076(9)	Mn3−O2−Mn2	111.06(15)
Mn3−O2	1.883(3)	Mn3−O2−Mn4	92.79(13)
Mn3−O5	1.887(3)	Mn2−O2−Mn4	125.40(17)
Mn3−O1	1.904(3)	Mn3−O5−Mn2	88.93(12)

Table 3. Bond Valence Sums for the Mn Atoms in Complex **1**[a]

atom	Mn^{II}	Mn^{III}	Mn^{IV}
Mn1	3.22	2.98	3.08
Mn2	3.13	2.89	2.99
Mn3	3.23	2.99	3.08
Mn4	3.20	2.92	3.07

[a] The underlined value is the one closest to the charge for which it was calculated, and the nearest whole number can be taken as the oxidation state of that atom.

The partially labeled structure and a stereoview of $[Mn_6O_4(OMe)_2(O_2CPh)_4(dphmp)_4]$ (**2**) are presented in Figure 2; selected interatomic distances and angles are listed in Table 4. Complex **2** crystallizes in the triclinic space group $P\bar{1}$, with two essentially superimposable independent molecules in the unit cell, both lying on inversion centers; only one will therefore be referred to below. The centrosymmetric molecule consists of a $[Mn_6O_4(OMe)_2]^{8+}$ core with peripheral ligation provided by six bridging $PhCO_2^-$ and four bidentate, chelating $dphmp^-$ groups. The core has a face-sharing double-cubane structure, containing two μ_3-O^{2-}, two μ_4-O^{2-},

(27) (a) Blackman, A. G.; Huffman, J. C.; Lobkovsky, E. B.; Christou, G. *Polyhedron* **1992**, *11*, 251. (b) Sun, Z.; Gantzel, P. K.; Hendrickson, D. N. *Inorg. Chem.* **1996**, *35*, 6640. (c) Lampropoulos, C.; Koo, C.; Hill, S. O.; Abboud, K.; Christou, G. *Inorg. Chem.* **2008**, *47*, 11180.

(28) (a) Vincent, J. B.; Christmas, C.; Chang, H.-R.; Li, Q.; Boyd, P. D. W.; Huffman, J. C.; Hendrickson, D. N.; Christou, G. *J. Am. Chem. Soc.* **1989**, *111*, 2086. (b) Christou, G. *Acc. Chem. Res.* **1989**, *22*, 328. (c) Libby, E.; McCusker, J. K.; Schmitt, E. A.; Folting, K.; Hendrickson, D. N.; Christou, G. *Inorg. Chem.* **1991**, *30*, 3486.

(29) Bouwman, E.; Bolcar, M. A.; Libby, E.; Huffman, J. C.; Folting, K.; Christou, G. *Inorg. Chem.* **1992**, *31*, 5185.

(30) (a) Brown, I. D.; Altermatt, D. *Acta Crystallogr.* **1985**, *B41*, 244. (b) Liu, W.; Thorp, H. H. *Inorg. Chem.* **1993**, *32*, 4102.

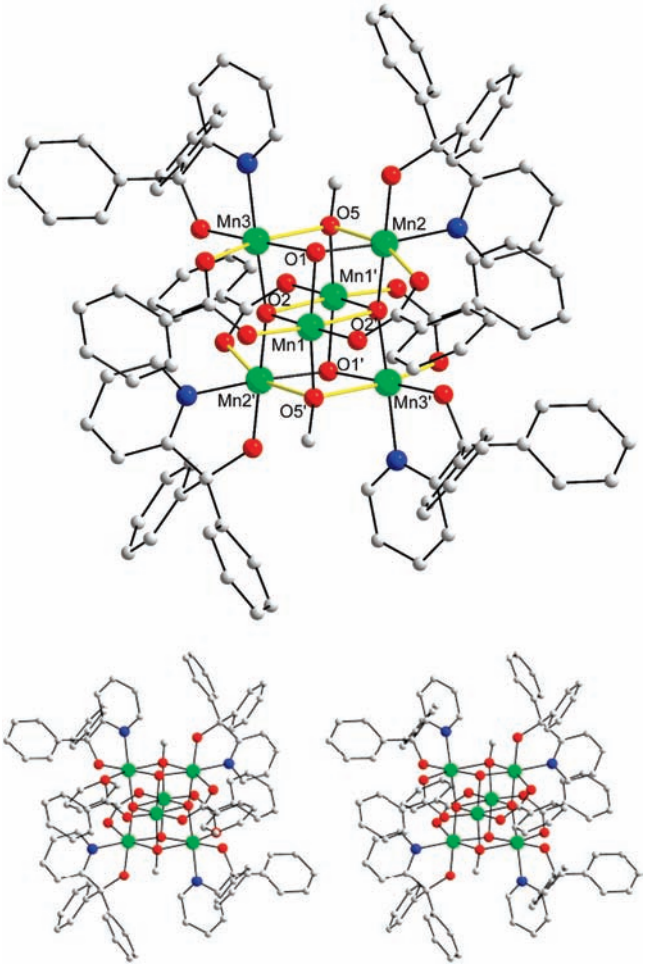

Figure 2. Structure of complex **2** with the Mn^{III} Jahn−Teller elongation axes shown as yellow bonds (top), and a stereopair (bottom). Hydrogen atoms have been omitted for clarity. Color code: Mn^{III} green; O red; N blue; C gray.

and two μ_3-MeO^- ions bridging the six Mn atoms. This is a very unusual and very rare structural type, and there has been only one previous report of a complex with this dicubane-like Mn_6 core, namely $[Mn_6O_4(OMe)_2(OAc)_4(Mesalim)_4]$ ($Mesalim^-$ = methyl salicylimidate anion).[31] The Mn atoms in **2** are all six-coordinate with near-octahedral geometry, and charge considerations and the metric parameters indicate they are all Mn^{III}, as confirmed by BVS calculations (Table 5). The Mn^{III} atoms thus all display JT axial elongations. Normally, the latter avoid Mn-oxide bonds, almost always the strongest and shortest in the molecule, but this is not possible for every Mn atom in **2** because of the double-cubane topology: for Mn2 and Mn3 (and their symmetry related partners), the JT axes are those containing the O atoms of the μ_3-MeO^- ions, but for Mn1 and Mn1′, the JT elongation axes contain a μ_4-O^{2-} ion O2′ or O2, respectively; the location of all JT axes are indicated as yellow bonds in Figure 2. The JT axes of Mn1, Mn1′, Mn3, and Mn3′ are oriented nearly parallel to each other, and perpendicular to those of Mn2 and Mn2′; they are thus all oriented in the xy planes, if the *z* axis is defined as the long axis of the

(31) Godbole, M. D.; Roubeau, O.; Mills, A. M.; Kooijman, H.; Spek, A. L.; Bouwman, E. *Inorg. Chem.* **2006**, *45*, 6713.

Table 4. Selected Interatomic Distances (Å) and Angles (deg) for **2**·3MeCN

Mn1−O1	1.918(6)	Mn3−O3	1.839(6)
Mn1−O5′	1.924(6)	Mn3−O2	1.924(6)
Mn1−O2	1.935(6)	Mn3−O1	1.925(6)
Mn1−O8	1.945(7)	Mn3−N1	2.037(8)
Mn1−O7	2.101(7)	Mn3−O6	2.267(7)
Mn1−O2′	2.390(7)	Mn3−O5	2.408(7)
Mn1···Mn3	2.803(2)	Mn3···Mn1′	3.208(2)
Mn1···Mn2	2.934(2)	Mn3−O2−Mn1	93.1(3)
Mn1···Mn2′	3.084(2)	Mn3−O2−Mn2′	161.4(3)
Mn1···Mn3′	3.208(2)	Mn1−O2−Mn2′	105.3(3)
Mn2−O4	1.851(6)	Mn3−O2−Mn1′	95.5(2)
Mn2−O1	1.938(6)	Mn1−O2−Mn1′	98.7(2)
Mn2−O2′	1.945(6)	Mn2′−O2-Mn1′	84.5(2)
Mn2−N2	2.030(8)	Mn1′−O5-Mn2	92.7(3)
Mn2−O9	2.240(7)	Mn1′−O5-Mn3	94.9(3)
Mn2−O5	2.319(7)	Mn2−O5−Mn3	88.2(2)
Mn2···Mn1′	3.084(2)		

Table 5. Bond Valence Sums for the Mn Atoms in Complex **2**[a]

atom	Mn^{II}	Mn^{III}	Mn^{IV}
Mn1	3.15	2.88	3.02
Mn2	3.15	2.91	3.00
Mn3	3.15	2.92	3.01

[a] See the footnote of Table 3.

double-cubane. There are no significant intermolecular interactions.

The complete structure and a stereoview of $[Mn_{11}O_7(OMe)_7(O_2CPh)_7(dphmp)_4(MeOH)_2]$ (**3**) are shown in Figure 3, and its labeled core is shown in Figure 4; selected interatomic distances and angles are listed in Table 6. Complex **3** possesses a $[Mn_{11}(\mu_4\text{-}O)_4(\mu_3\text{-}O)_5(\mu\text{-}OR)_6]$ core containing four μ_4-O^{2-} (O30, O31, O33, and O34), three μ_3-O^{2-} (O28, O29 and O32), two μ_3-MeO^- (O17 and O19), five μ-MeO^- (O18, O20, O21, O22, and O25), and one μ-RO^- alkoxide arm (O1) of a $\eta^1{:}\eta^2{:}\mu$-$dphmp^-$ group that is chelating on Mn2 and bridging to Mn3 in a very asymmetric manner (Mn2−O1 = 1.879(1) Å vs Mn3−O1 = 2.415(2) Å). The other three $dphmp^-$ groups are bound as η^2 chelates. Six of the seven benzoates are bridging two Mn^{III} atoms in the common $\eta^1{:}\eta^1{:}\mu$-bridging mode, and the seventh is bound terminally to Mn^{II} atom Mn11 and hydrogen-bonds to one of the two terminal MeOH groups on Mn11 that complete the ligation. The Mn oxidation states were deduced from charge considerations and the metric parameters, and confirmed by BVS calculations (Table 7).

The core of **3** can be described as consisting of a $[Mn_4O_3(OMe)]$ cubane (Mn4, Mn7, Mn8, and Mn9) linked on one side to the Mn^{II} atom (Mn11) by a cubane O^{2-} and two μ-MeO^- groups. On the other side, the cubane face is linked to a $[Mn_5O_7]$ unit which can be described as a central $[Mn_4O_3]$ defective cubane (Mn2, Mn3, and Mn5) sharing two of its faces with two other defective cubanes (Mn1, Mn2, Mn5 and Mn3, Mn5, Mn6), the latter of which is linked by μ_3-O^{2-} ion O28 to another Mn atom (Mn10) that is also attached to the cubane by a μ-MeO^- group. It is thus interesting that **3** bears some structural similarity to **2** in containing a cubane unit. Complex **3** is the first example of this low symmetry Mn_{11} topology, and in fact joins only a

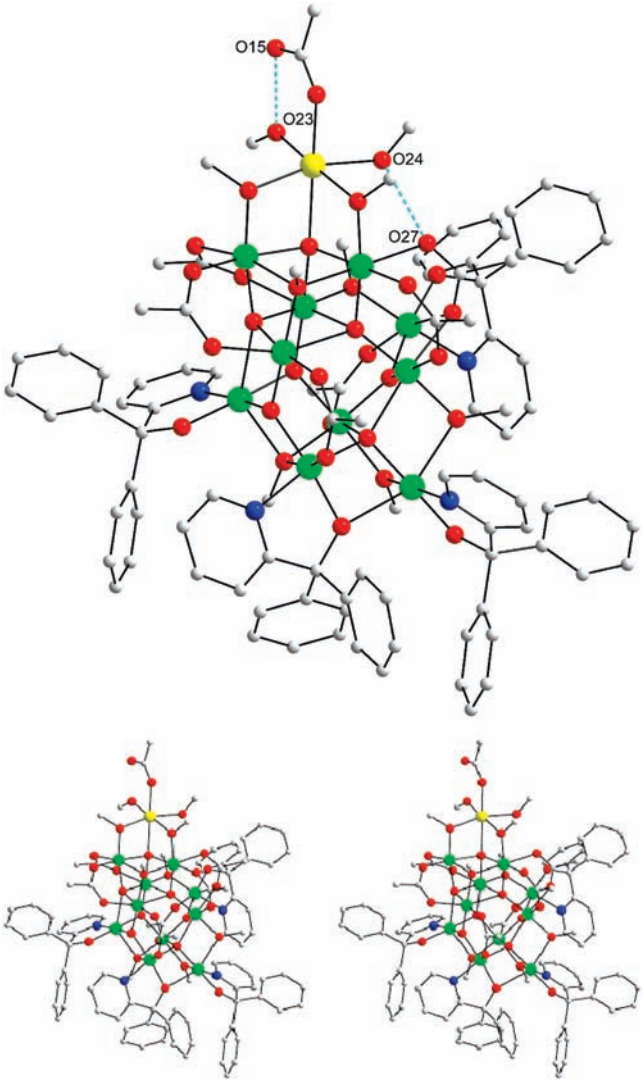

Figure 3. Structure of complex **3** with intramolecular hydrogen-bonds shown as dashed lines (top), and a stereopair (bottom). Hydrogen atoms and benzoate phenyl rings (except for the *ipso* carbon atoms) have been omitted for clarity. Color code: Mn^{II} yellow; Mn^{III} green; O red; N blue; C gray.

very small family of Mn/O clusters with a nuclearity of 11.[32]

Magnetochemistry. dc Magnetic Susceptibility of Complexes 1−3. Variable temperature magnetic susceptibility measurements were performed on microcrystalline powder samples of complexes **1**·2MeCN·H_2O, **2**·2H_2O, and **3** in a 1 kOe (0.1 T) dc field and in the 5.0−300 K range. The samples were restrained in eicosane to prevent torquing in the applied field. The obtained data for **1-3** are shown as $\chi_M T$ versus T plots in Figures 5−7, respectively.

For complex **1**·2MeCN·H_2O, $\chi_M T$ gradually decreases from 7.57 cm^3 K mol^{-1} at 300 K to 4.99 cm^3 K mol^{-1} at 40.0 K and then decreases more rapidly to 1.72 cm^3 K mol^{-1} at 5.0 K (Figure 5). The 300 K value is much smaller than the spin-only ($g = 2$) value of 12 cm^3 K mol^{-1} for four noninteracting Mn^{III} atoms, indicating the presence of dominant antiferromagnetic exchange

(32) (a) Perlepes, S. P.; Huffman, J. C.; Christou, G. *J. Chem. Soc., Chem. Commun.* **1991**, 1657. (b) Murugesu, M.; Wernsdorfer, W.; Abboud, K. A.; Christou, G. *Polyhedron* **2005**, *24*, 2894.

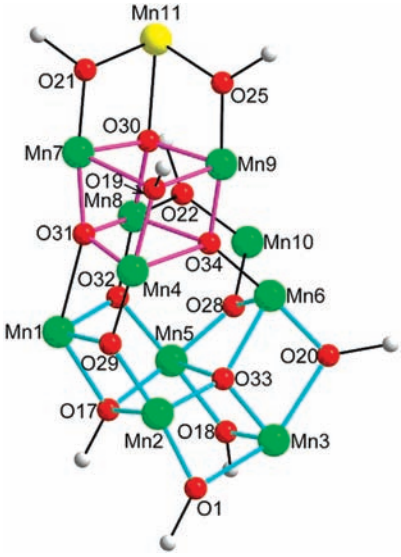

Figure 4. Fully labeled core of complex **3**. Color code: Mn^{II} yellow; Mn^{III} green; O red; C gray.

Table 6. Selected Interatomic Distances (Å) for **3**·4MeCN

Mn1−O2	1.850(3)	Mn6−O13	1.996(3)
Mn1−O32	1.892(3)	Mn6−O33	2.160(3)
Mn1−O29	1.948(3)	Mn6−O26	2.279(3)
Mn1−N2	2.044(4)	Mn7−O21	1.881(3)
Mn1−O17	2.185(3)	Mn7−O31	1.903(3)
Mn1−O31	2.442(3)	Mn7−O8	1.993(3)
Mn2−O33	1.873(3)	Mn7−O30	2.010(3)
Mn2−O29	1.878(3)	Mn7−O9	2.082(3)
Mn2−O1	1.879(3)	Mn7−O19	2.268(3)
Mn2−N1	2.041(4)	Mn8−O32	1.900(3)
Mn2−O5	2.219(3)	Mn8−O30	1.925(3)
Mn2−O17	2.422(3)	Mn8−O22	1.944(3)
Mn3−O3	1.862(3)	Mn8−O31	1.964(3)
Mn3−O33	1.907(3)	Mn8−O34	2.191(3)
Mn3−O18	1.929(3)	Mn8−O10	2.242(3)
Mn3−N3	2.045(4)	Mn9−O34	1.874(3)
Mn3−O20	2.247(3)	Mn9−O25	1.893(3)
Mn3−O1	2.415(3)	Mn9−O14	1.962(3)
Mn4−O29	1.864(3)	Mn9−O30	1.965(3)
Mn4−O31	1.914(3)	Mn9−O19	2.217(3)
Mn4−O6	1.933(3)	Mn9−O27	2.266(3)
Mn4−O19	1.942(3)	Mn10−O4	1.862(3)
Mn4−O7	2.241(3)	Mn10−O28	1.872(3)
Mn4−O34	2.444(3)	Mn10−O22	1.938(3)
Mn5−O28	1.843(3)	Mn10−N4	2.041(3)
Mn5−O32	1.895(3)	Mn10−O12	2.219(3)
Mn5−O17	1.941(3)	Mn10−O26	2.308(3)
Mn5−O18	2.000(3)	Mn11−O25	2.121(3)
Mn5−O11	2.116(3)	Mn11−O16	2.128(4)
Mn5−O33	2.395(3)	Mn11−O21	2.131(3)
Mn6−O34	1.880(3)	Mn11−O23	2.174(4)
Mn6−O20	1.910(3)	Mn11−O24	2.241(4)
Mn6−O28	1.949(3)	Mn11−O30	2.293(3)

interactions within the molecule. $\chi_M T$ is clearly heading for zero at the lowest temperatures, indicating that complex **1** possesses an $S = 0$ ground state. Because of this and the low symmetry of the molecule, which requires five separate Mn_2 pairwise exchange parameters (J_{ij}) to describe its exchange coupling (and more if interactions with next-nearest neighbors are included), we did not pursue fits of the $\chi_M T$ versus T data by matrix diagonalization to determine the values of the exchange interactions. Unfortunately, the more convenient Kambe vector

Table 7. Bond Valence Sums for the Mn Atoms in Complex **3**[a]

atom	Mn^{II}	Mn^{III}	Mn^{IV}
Mn1	3.18	2.95	3.04
Mn2	3.28	3.03	3.13
Mn3	3.13	2.89	2.98
Mn4	3.12	2.86	3.00
Mn5	3.23	2.96	3.11
Mn6	3.15	2.88	3.02
Mn7	3.16	2.89	3.03
Mn8	3.14	2.87	3.01
Mn9	3.17	2.90	3.05
Mn10	3.26	3.02	3.12
Mn11	1.98	1.81	1.90

[a] See footnote of Table 3.

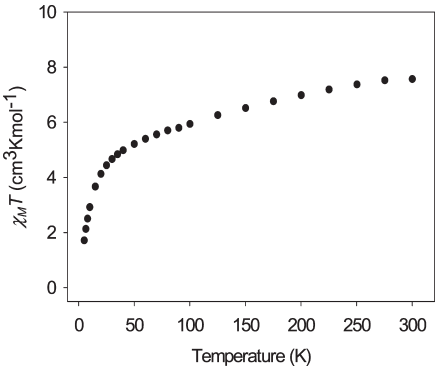

Figure 5. Plot of dc $\chi_M T$ vs T for complex **1**.

coupling method[33] cannot be applied to such a low symmetry molecule. In any case, the exchange interactions are expected to be weak, based on the many previous magnetic studies of such molecules that we have reported, making accurate determinations of so many independent J values problematic, to say the least.

For complex **2**·2H_2O, $\chi_M T$ gradually decreases from 13.8 cm^3 K mol^{-1} at 300 K to 6.64 cm^3 K mol^{-1} at 5.0 K (Figure 6). The 300 K value is again much smaller than the spin-only ($g = 2$) value of 18 cm^3 K mol^{-1} for six noninteracting Mn^{III} atoms, indicating the presence of at least some strong antiferromagnetic interactions. However, the plot is clearly not heading to zero at 0 K, indicating that **2** has a ground state with $S > 0$, and the 5.0 K value is close to the spin-only value of 6.00 cm^3 K mol^{-1} expected for an $S = 3$ ground state. Although complex **2** is more symmetric than **1**, it is still not possible to apply the Kambe method for fitting the $\chi_M T$ versus T data. We thus chose to confirm the ground state by ac studies, as will be described below (vide infra).

For complex **3**, $\chi_M T$ steadily decreases from 29.4 cm^3 K mol^{-1} at 300 K to 19.9 cm^3 K mol^{-1} at 50.0 K, and then decreases more rapidly to 8.14 cm^3 K mol^{-1} at 5.0 K (Figure 7). The 300 K value is once more much smaller than the spin-only value of 34.4 cm^3 K mol^{-1} for 1 Mn^{II} and 10 Mn^{III} noninteracting atoms indicating the presence of dominant antiferromagnetic interactions. As for **2**·2H_2O, the $\chi_M T$ at 5.0 K of **3** is not heading for zero at 0 K, indicating an $S > 0$ ground state, and the value at 5 K can be compared with the spin-only ($g = 2$) values of 4.38

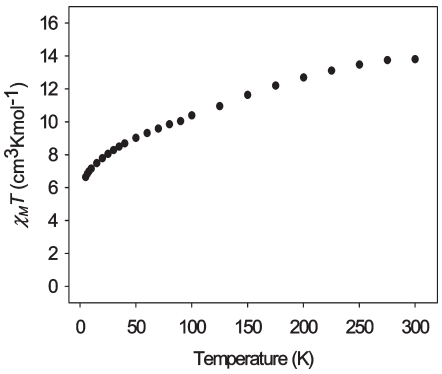

Figure 6. Plot of dc $\chi_M T$ vs T for complex **2**.

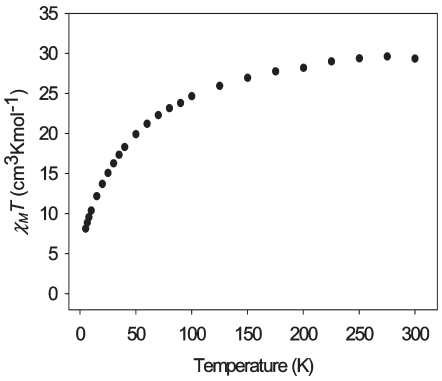

Figure 7. Plot of dc $\chi_M T$ vs T for complex **3**.

and 7.88 cm^3 K mol^{-1} expected for $S = 5/2$ and 7/2 states, respectively.

We attempted to confirm the ground state estimates for **2** and **3** from fits of variable-field (H) and -temperature magnetization (M) data collected in the 0.1−7 T and 1.8−10 K ranges. Attempts to fit the data were made, using the program MAGNET,[34] by diagonalization of the spin Hamiltonian matrix assuming only the ground state is populated, incorporating axial anisotropy ($D\hat{S}_z^2$) and Zeeman terms, and employing a full powder average. The corresponding spin Hamiltonian is given by eq 4, where $\hat{S}_z$ is the easy-axis spin operator, g is the

$$\mathscr{H} = D\hat{S}_z^2 + g\mu_B\mu_0\hat{S}\cdot H \quad (4)$$

Landé g factor, μ_B is the Bohr magneton, and μ_0 is the vacuum permeability. However, for neither **2** nor **3** were we able to obtain a satisfactory fit. This is not unusual in Mn_x cluster chemistry and is almost always because of the presence of low-lying excited states because (i) the excited states are close enough to the ground state that they are populated even at very low temperatures, and/or (ii) even higher-lying excited states whose S is greater than that of the ground-state become populated as their larger M_S levels rapidly decrease in energy in the applied dc field and approach (or even cross) those of the ground state. Either (or both) of these two effects will lead to poor fits because the fitting program assumes population of only the ground state. The presence of low-lying excited states is

(33) Kambe, K. *J. Phys. Soc. Jpn.* **1950**, *5*, 48.

(34) Davidson, E. R. *MAGNET*; Indiana University: Bloomington, IN, 1999.

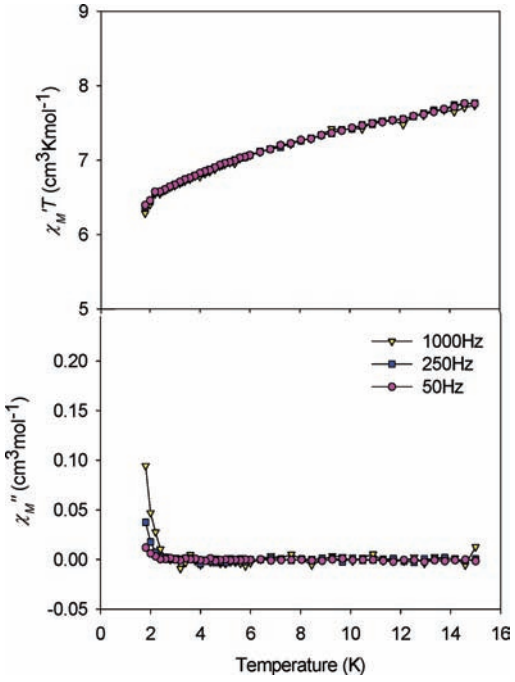

Figure 8. ac susceptibility of complex **2** in a 3.5 Oe field oscillating at the indicated frequencies: (top) in-phase (χ_M') signal, plotted as $\chi_M'T$ vs T; (bottom) out-of-phase (χ_M'') signal vs T.

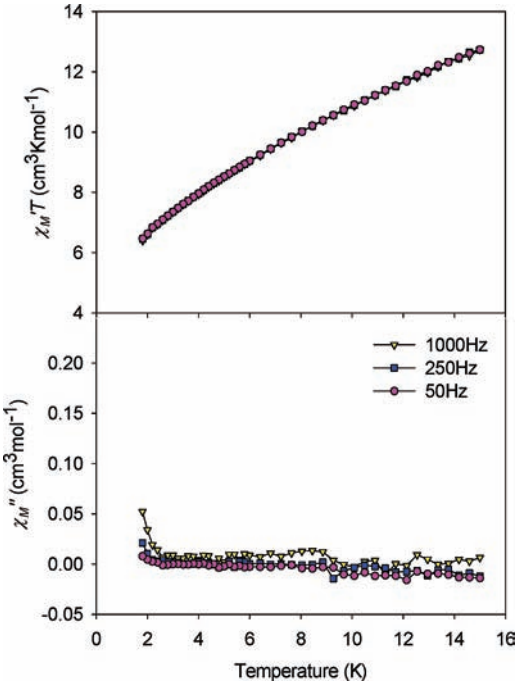

Figure 9. ac susceptibility of complex **3** in a 3.5 Oe field oscillating at the indicated frequencies: (top) in-phase (χ_M') signal, plotted as $\chi_M'T$ vs T; (bottom) out-of-phase (χ_M'') signal vs T.

evident in the magnetization (M) versus field (H) data at 2 K, and the corresponding M versus H/T data, neither of which show saturation but instead a steadily increasing M with H (see Supporting Information). We can normally get around problem (ii) by employing only data collected in small fields and/or lower temperatures,[27c,35] but for **2** and **3** we still could not get good fits even with data at < 1 T and < 5 K. We conclude that the **2** and **3** have very low-lying excited states, and we therefore turned to ac susceptibility measurements as an alternative means to determine their ground states.

Ac Magnetic Susceptibility of Complexes 2 and 3. The ac susceptibility studies are a powerful complement to dc studies for determining the ground state spin of a system because they preclude complications arising from the presence of a dc field. They were performed for **2** and **3** in the 1.8−15 K range using a 3.5 Oe ac field oscillating at frequencies in the 50−1000 Hz range. For **2**, the obtained in-phase (χ_M', plotted as $\chi_M'T$) and out-of-phase (χ_M'') ac susceptibility data are shown in Figure 8. In the absence of slow magnetization relaxation and a resulting out-of-phase signal, the ac $\chi_M'T$ is equal to the dc $\chi_M'T$ and thus allows determination of the ground state S in the absence of a dc field. The $\chi_M'T$ versus T plot of Figure 8 (top) decreases significantly with decreasing temperature indicating population of one or more excited states and rationalizing the problematic fits of dc magnetization data. In particular, a decreasing $\chi_M'T$ versus T plot with decreasing T is indicative of the population of low-lying excited states with S values greater than the ground-state S. Extrapolation of the plot from above 4 to 0 K, where only the ground state will be populated, gives a $\chi_M'T$ value of $\sim$6 cm^3 K mol^{-1}, which is the value expected for an $S = 3$ state with $g \sim 2.0$. This conclusion is the same as that reached from the dc study, and provides an independent confirmation that complex **2** possesses an $S = 3$ ground state.

The out-of-phase (χ_M'') susceptibility in Figure 8 (bottom) is zero until $\sim$3 K, and then shows a small frequency-dependent rise. If the magnetization vector relaxes fast enough to keep up with the oscillating ac field, there will be no χ_M'' signal, but if the relaxation barrier is significant compared to thermal energy (kT), then there is a non-zero χ_M'' signal and the in-phase signal decreases. In addition, the χ_M'' signal and the decrease in the $\chi_M'T$ signal will both be frequency-dependent. Such frequency-dependent ac signals are an indication of the superparamagnet-like slow relaxation of a SMM. The χ_M'' signal in Figure 8 is weak and parallels a tiny drop in the in-phase $\chi_M'T$; nevertheless, the $\chi_M''/\chi_M'T$ ratio is small ($\sim$1.5%), and the χ_M'' signal is clearly just the small tail of a much stronger χ_M'' peak whose maximum is below the 1.8 K operating limit of our SQUID magnetometer. The data may be indicating that complex **2** exhibits the slow magnetization relaxation dynamics of a SMM, but with only a very small barrier; however, since we cannot see much of the peak down to 1.8 K, we cannot be sure that it is not arising from an impurity. It would require single-crystal micro-SQUID studies down to 40 mK to better explore the possible SMM properties, but these were not pursued given the only small barrier evident and the many such studies on other SMMs with small barriers already reported.

For **3**, the in-phase $\chi_M'T$ and out-of-phase χ_M'' data are shown in Figure 9. The $\chi_M'T$ versus T plot in Figure 9 (top) decreases very rapidly with decreasing temperature, supporting a very high density of low-lying excited states consistent with the higher nuclearity of this complex and

(35) (a) Soler, M.; Wernsdorfer, W.; Folting, K.; Pink, M.; Christou, G. *J. Am. Chem. Soc.* **2004**, *126*, 2156. (b) Sanudo, E. C.; Wernsdorfer, W.; Abboud, K. A.; Christou, G. *Inorg. Chem.* **2004**, *43*, 4137.

Table 8. Complexes with hmp^- or $dphmp^-$, and the Alkoxide O Atom Binding Mode

complex[a]	n (μ_n-O)[b]	ref
$[Mn_4O_2(O_2CPh)_7(hmp)_2]^-$	1	28
$[Mn_4(hmp)_6X_{4-x}(solv)_x]^{z+}$ [c]	3	25,26 6
$[Mn_4(6\text{-Me-hmp})_6Cl_4]$	3	25a
$[Mn_4(hmp)_4Br_2(OMe)_2(dcn)_2]$	3	25c
$[Mn_4(hmp)_4(acac)_2(MeO)_2]^{2+}$	2	36
$[Mn_7(OH)_3(hmp)_9Cl_3]^{2+}$	2, 3	19
$[Mn_{10}O_4(OH)_2(O_2CMe)_8(hmp)_8]^{4+}$	2, 3	19a
$[Mn_{10}O_4(N_3)_4(hmp)_{12}]^{2+}$	2	37
$[Mn_{12}O_8Cl_4(O_2CPh)_8(hmp)_6]$	2	38
$[Mn_{21}O_{14}(OH)_2(O_2CMe)_{16}(hmp)_8(pic)_2(py)(H_2O)]^{4+}$	2	39
$[Mn_4O_2(O_2CBu^t)_5(dphmp)_3]$ (**1**)	1, 2	t.w.
$[Mn_6O_4(OMe)_2(O_2CPh)_4(dphmp)_4]$ (**2**)	1	t.w.
$[Mn_{11}O_7(OMe)_7(O_2CPh)_7(dphmp)_4(MeOH)_2]$ (**3**)	1, 2	t.w.

[a] Counterions omitted. [b] Bridging mode of the hmp^- or $dphmp^-$ O atom; μ_1-O indicates a nonbridging (terminal) mode. [c] Many complexes, varying in the content of monodentate anionic ligand X^- and solvent molecules (solv). t.w. = this work.

again rationalizing the unsatisfactory fits of dc magnetization data. The steeply decreasing and curving plot makes extrapolation to 0 K trickier and more unreliable, but it appears to be heading for a $\chi_M'T$ value in the 4−5 cm^3 K mol^{-1} range, which is clearly pointing to an $S = 5/2$ ground state (4.38 cm^3 K mol^{-1} for $g = 2$) rather than an $S = 3/2$ (1.88 cm^3 K mol^{-1}) or $S = 7/2$ (7.88 cm^3 K mol^{-1}) ground state. We thus conclude that complex **3** has an $S = 5/2$ ground state. Below ~3 K, there is a small dip in the $\chi_M'T$ signal concomitant with the appearance of a frequency-dependent χ_M'' signal (Figure 9, bottom). Assuming the latter weak signal is not because of an impurity, this would point to **3** perhaps being an SMM, but again one with only a very small barrier, and we thus did not pursue further characterization.

Comparison of $dphmp^-$ and hmp^- Mn Clusters. The initial objective of this work was to explore whether the introduction of bulky phenyl substituents at the CH_2 position of hmpH might lead to products distinctly different from those previously obtained from hmpH, and this has been found to be the case. None of the products obtained to date containing bulky $dphmp^-$ are structurally the same as those obtained previously with hmp^-. Instead, all three products of the present study have been found to be prototypical or very rare structural types in Mn cluster chemistry. However, Mn chemistry is already known to be amazingly fickle, with obtained products often changing dramatically when reaction conditions such as the identity of the solvent or the carboxylate are changed (for reasons discussed above). Thus, the simple fact that $dphmp^-$ gives different products from hmp^- is not in itself so surprising. A much more pertinent and useful question to ask is whether there is anything systematically different between the products with $dphmp^-$ and hmp^-? The answer is yes: the $dphmp^-$ and hmp^- are exhibiting distinctly different binding modes that can be directly assigned to the presence of the Ph groups and which consequently lead to the different structural types of products. The various types of known Mn clusters containing hmp^- are listed in Table 8, together with complexes **1**−**3** from this work, and the binding modes of the alkoxide O atom. Immediately apparent is a strong tendency of the hmp^- alkoxide arm to bridge two Mn atoms, and even three Mn atoms in most of the $[Mn_4(hmp)_6]^{4+}$- and $[Mn_4(hmp)_4]^{6+}$-containing complexes, as well as $[Mn_7(OH)_3(hmp)_9Cl_3]^{2+}$ and $[Mn_{10}O_4(OH)_2(O_2CMe)_8(hmp)_8]^{4+}$.[19,25,26] The carboxylate-rich anion $[Mn_4O_2(O_2CPh)_7(hmp)_2]^-$ is the exception that proves the rule in containing only chelating hmp^- groups. This preference of the numerous hmp^- groups in these many complexes to almost all favor a bridging mode for their alkoxide group is as expected for mid- and late-transition metals. The same is seen for Fe/hmp^- chemistry, although we restrict the present discussion to Mn. In contrast, 9 of the 11 $dphmp^-$ groups in complexes **1**−**3** bind in non-bridging, chelate modes. For the 10th and 11th, even these ostensibly bridging $dphmp^-$ groups bridge very asymmetrically, as described above (complex **1**: Mn3−O5 = 1.887(3) vs Mn2−O5 = 2.505(3) Å; complex **3**: Mn2−O1 = 1.879(1) Å vs Mn3−O1 = 2.415(2) Å), and perhaps are best described as semi-bridging. Thus, although the number of $dphmp^-$ products is admittedly limited to date, we believe the trend is nevertheless clear: the influence of the two bulky Ph groups next to the alkoxide O atom disfavors adoption of a bridging mode. We believe this is primarily due to steric effects, but there will also be an electronic effect of the electron-withdrawing Ph groups lowering the basicity of the O atom. Thus, with $dphmp^-$ favoring a chelating mode, it is not surprising that its Mn clusters are distinctly different from those obtained with hmp^-. It now also makes sense that the Mn_6 core of complex **2** is the same as that found previously in $[Mn_6O_4(OMe)_2(OAc)_4(Mesalim)_4]$, where the $Mesalim^-$ anion is a bidentate chelate.

Conclusions

The introduction of two bulky phenyl groups onto the CH_2 group of hmp^- has proven to be a route to new Mn clusters not accessible with hmp^- itself, and with prototypical or very rare structures. In contrast to hmp^-, the bulkier $dphmp^-$ favors a chelating, non-bridging binding mode. As a result, products are readily obtained with other bridging ligands such as carboxylates filling up coordination sites. This is in contrast to hmp^-, which favors chelating/bridging binding modes and whose higher denticity will often preclude the incorporation of additional bridging groups such as carboxylates. The reluctance of $dphmp^-$ to adopt a bridging mode is clearly due to the nearby steric bulk of the two Ph groups, and perhaps their electron-withdrawing effect on the O atom. This

(36) Yang, E.-C.; Harden, N.; Wernsdorfer, W.; Zakharov, L. N.; Brechin, E. K.; Rheingold, A. L.; Christou, G.; Hendrickson, D. N. *Polyhedron* **2003**, *22*, 1857.
(37) (a) Stamatatos, Th. C.; Abboud, K. A.; Wernsdorfer, W.; Christou, G. *Angew. Chem., Int. Ed.* **2006**, *45*, 4134. (b) Stamatatos, T. C.; Poole, K. M.; Abboud, K. A.; Wernsdorfer, W.; O'Brien, T. A.; Christou, G. *Inorg. Chem.* **2008**, *47*, 5006.
(38) (a) Boskovic, C.; Brechin, E. K.; Streib, W. E.; Folting, K.; Hendrickson, D. N.; Christou, G. *Chem. Commun.* **2001**, 467. (b) Boskovic, C.; Brechin, E.; Streib, W. E.; Folting, K.; Bollinger, J. C.; Hendrickson, D. N.; Christou, G. *J. Am. Chem. Soc.* **2002**, *124*, 3725.
(39) Sanudo, E. C.; Brechin, E. K.; Boskovic, C.; Wernsdorfer, W.; Yoo, J.; Yamaguchi, A.; Concolino, T. R.; Abboud, K. A.; Rheingold, A. L.; Ishimoto, H.; Hendrickson, D. N.; Christou, G. *Polyhedron* **2003**, *22*, 2267.

raises the obvious question of whether the binding mode, and thus the identity of the obtained Mn clusters, can be altered in a targeted way by modifying the size and electronic effects of the two substituents. This is currently under systematic investigation, and the results will be reported in due course.

Acknowledgment. We thank the National Science Foundation (CHE-0910472) for support of this work.

Supporting Information Available: X-ray crystallographic data in CIF format for complexes **1**·2MeCN, **2**·3MeCN, and **3**·4MeCN. This material is available free of charge via the Internet at http://pubs.acs.org.